Received: 9 April 2018 | Revised: 3 July 2018 | Accepted: 9 July 2018

DOI: 10.1111/bre.12309

ORIGINAL ARTICLE

WILEY Basin Research IAS EAGE

Novel discrete element modelling of Gilbert-type delta formation in an active tectonic setting—first results

Stuart Hardy[1,2]

[1]ICREA (Institució Catalana de Recerca i Estudis Avançats), Barcelona, Catalonia, Spain

[2]Facultat de Geologia, Universitat de Barcelona, Barcelona, Catalonia, Spain

Correspondence
Stuart Hardy, ICREA (Institució Catalana de Recerca i Estudis Avançats), Passeig Lluís Companys 23. 08010 Barcelona, Catalonia, Spain.
Email: stuart.hardy@icrea.cat

Abstract

Gilbert deltas are now recognised as an important stratigraphic component of many extensional basins. They are remarkable due to their coarse-grained nature, large size and steep foresets (up to 30–35°) and may exhibit a variety of slope instability features (faulting, slump scars, avalanching, etc.). They are also often closely related to major, basin-margin normal faults. There has been considerable research interest in Gilbert deltas, partly due to their economic significance as stratigraphic traps for hydrocarbons but also due to their sensitivity to relative base level changes, giving them an important role in basin analysis. In addition to field studies, numerical modelling has also been used to simulate such deltas, with some success. However, until now, such studies have typically employed continuum numerical techniques where the basic data elements created by simulations are stratigraphic volumes or timelines and the sediments themselves have no internal properties *per se* and merely represent areas/volumes of introduced coarse-grained, clastic and sedimentary material. Faulting or folding (if present) are imposed externally and do not develop (naturally) within the modelled delta body itself. Here, I present first results from a novel 2D numerical model which simulates coarse-grained (Gilbert-type) deltaic sedimentation in an active extensional tectonic setting undergoing a relative base level rise. Sediment is introduced as packages of discrete elements which are deposited beneath sea level, from the shoreline, upon a pre-existing basin or delta. These elements are placed carefully and then allowed to settle onto the system. The elements representing the coarse-grained, deltaic sediments can have an intrinsic coefficient of friction, cohesion or other material properties appropriate to the system being considered. The spatial resolution of the modelling is of the order of 15 m and topsets, foresets, bottomsets, faults, slumps and collapse structures all form naturally in the modelled system. Examples of deltas developing as a result of sediment supply from both the footwall and hanging-wall of a normal fault, and subject to changes in fault slip rate are presented. Implications of the modelling approach, and its application and utility in basin research, are discussed.

1 | INTRODUCTION

Sedimentary basins are rarely simple and much of their complexity arises from the structural and stratigraphic heterogeneity of the upper crustal section being deformed. This makes the interpretation of preserved sedimentary deposits, and the understanding of controlling factors, difficult and at times complex. In extensional (rift) basins, Gilbert-type deltas (Gilbert, 1885, 1890) are an important component of the stratigraphy and have been recognised in both active and ancient basins; they are remarkable due to their coarse-grained nature, large size, steep forests (up to 30–35°) and their close association with major normal faults (e.g., Backert, Ford, & Malartre, 2010; Colella, 1988a; Dart, Collier, Gawthorpe, Keller, & Nichols, 1994; Malartre, Ford, & Williams, 2004; Figure 1a,b). They consist typically of a wedge-shaped body of coarse-grained sediments, comprising relatively thin, flat-lying topsets, long, steeply-dipping foresets, and thinner, more flat-lying, bottomset deposits (Figure 1a). As they form at basin margins, they are often visible in the present day and in exhumed basins. As a result, they have been the focus of many field studies (e.g., Colella, 1988a,b; Dart et al., 1994; Fernandez & Guerra-Merchan, 1996; Ford, Williams, Malartre, & Popescu, 2007; Garcia-Garcia, Fernandez, Viseras, & Soria, 2006; Malartre et al., 2004; Figure 1b). The considerable research interest in Gilbert deltas is partly due to their economic significance as stratigraphic traps for hydrocarbons, but is also due to their sensitivity to relative base level changes, giving them an important role in basin analysis. Numerical modelling has also been used to simulate such deltas, with some success (e.g., Hardy, Dart, & Waltham, 1994; Hardy & Gawthorpe, 1998; Ritchie, Gawthorpe, & Hardy, 2004a,b; Ritchie, Hardy, & Gawthorpe, 1999). However, such studies have typically employed continuum numerical techniques where the basic data elements used/stored by simulations are stratigraphic timelines and the modelled sediments themselves have no properties *per se* and merely represent timelines/volumes of introduced clastic materials (cf. Figure 1c). Sedimentary processes in the water column may be modelled with a high degree of complexity, with facies being recorded, but after the sediments are deposited little happens *within* the sedimentary body, excluding compaction perhaps (e.g., Gratacos, Bitzer, Cabrera, & Roca, 2009). Thus, these simulations usually only impose faulting/subsidence as an external boundary condition and the delta itself does not deform internally or slump/collapse, for example, under its own weight or if the delta front is over-steepened. These limitations place a major constraint on our ability to better interpret or understand Gilbert delta geometries seen in the field by comparison to such simulations. Here, I present the first results of a novel 2D discrete element model which simulates coarse-grained (Gilbert-type) deltaic sedimentation in an extensional tectonic setting. In these initial results, I do not consider the delivery of sediment to the shoreline or any erosion during relative base level fall. Sediment is simply introduced periodically as small packages of discrete elements which are deposited beneath sea level upon a pre-existing basin topography or a growing delta. These elements are then allowed to settle onto the system (Figure 1d). The elements representing the coarse-grained deltaic sediments can have an intrinsic coefficient of friction, cohesion or other material properties appropriate to the system being considered. The spatial resolution of the modelling is of the order of 15 m and typical Gilbert delta profiles are produced with faults, collapse/slump structures, etc., all forming naturally in the modelled deltas. I will present experiments that simulate deltas developing as a result of sediment supply from the footwall of a simple normal fault (Figure 2), hanging wall-derived deltas being deposited onto a tilting hanging-wall surface which is either frictional or frictionless (Figures 3 and 4), and a footwall-derived delta with a changing slip history through time (Figures 5 and 6). In all cases, the deltas are subject to a relative base level rise. The implications of the modelling approach, its application and utility in basin research, and further potential developments, are discussed.

2 | METHODOLOGY

Here, I use a discrete element numerical model to simulate coarse-grained, Gilbert-type, deltas in an active tectonic setting. The discrete element code used here to undertake these simulations is "cdem2D" which has been used previously to undertake a wide variety of structural geology modelling in both 2D and 3D. The basic numerical methodology and its application to a variety of problems (fault-propagation folding, orogenic wedge growth, caldera collapse, dike intrusion on Mars, viscous flow, etc.) have been published previously (e.g., Botter, Cardozo, Hardy, Lecomte, & Escalona, 2014; Botter et al., 2016; Hardy, 2008, 2016, 2018; Hardy, McClay, & Muñoz, 2009). Of particular interest here, the details of this code applied to granular, frictional materials can be found elsewhere (e.g., Hardy, 2011, 2015; Hardy et al., 2009), however, an overview is given below. In all previous studies, the code has been used to simulate deformation of a *pre-existing* sedimentary cover. Here, I will illustrate the use of this modelling scheme to simulate sedimentation *per se* and any internal deformation of the resultant sedimentary body.

Discrete element models, in common with other numerical techniques, have both advantages and disadvantages when considering their application to a geological

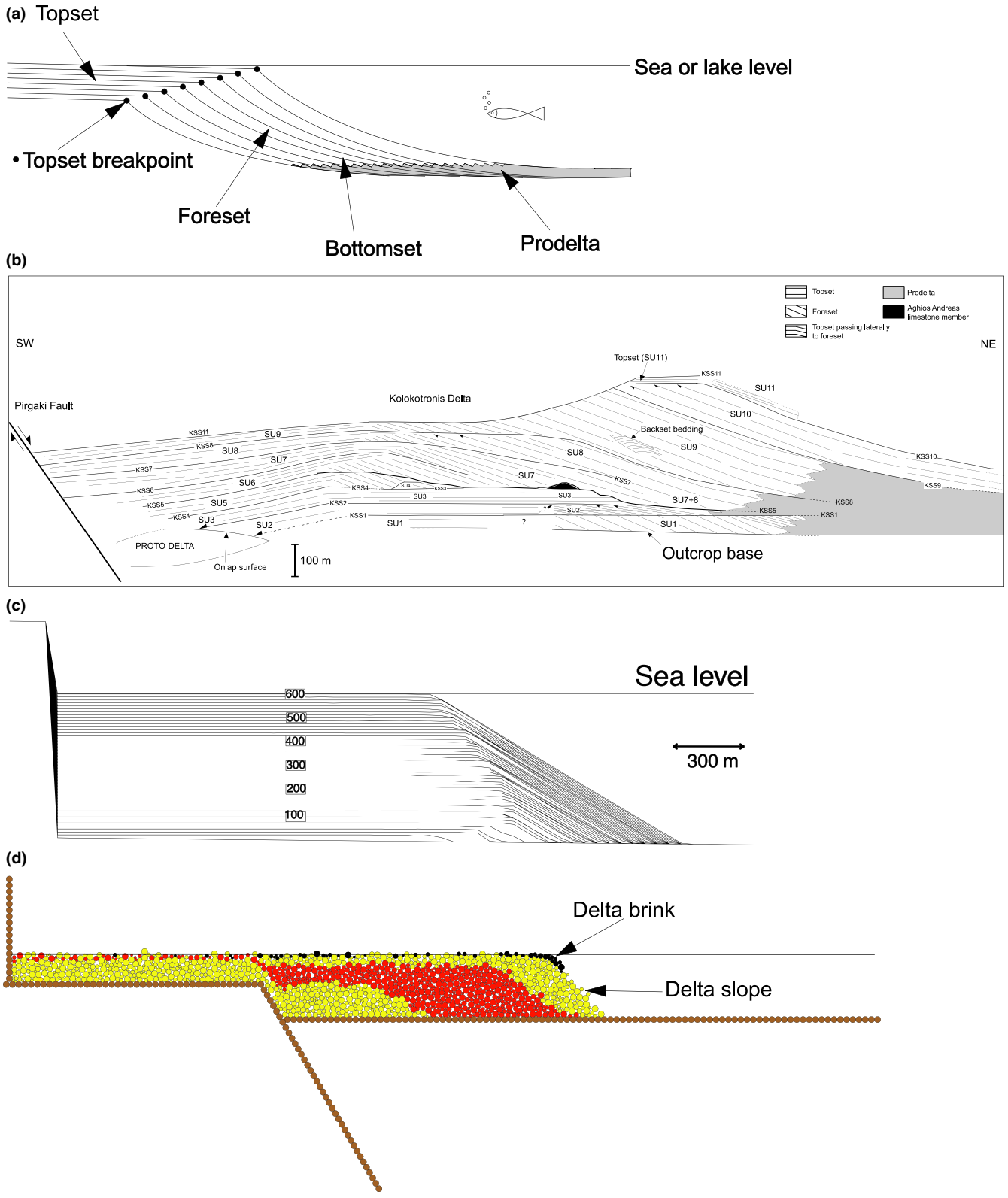

FIGURE 1 (a) Schematic diagram illustrating main elements of Gilbert-type deltas. (b) Synthetic north-east to south-west cross-section through the Kerinitis Delta, Gulf of Corinth showing the key stratal surfaces (KSS) and stratal units (SU) (redrawn from Backert et al., 2010). (c) Numerical model of a Gilbert delta developed over 600 ka with constant sediment supply, redrawn from Hardy and Gawthorpe (2002), note the lack of faulting or any internal structure within the delta body. (d) Snapshot of the numerical model presented here immediately after adding a package of discrete elements representing new coarse-grained sediments (shown in black) and allowing them to settle on the existing Gilbert delta body (yellow and red)

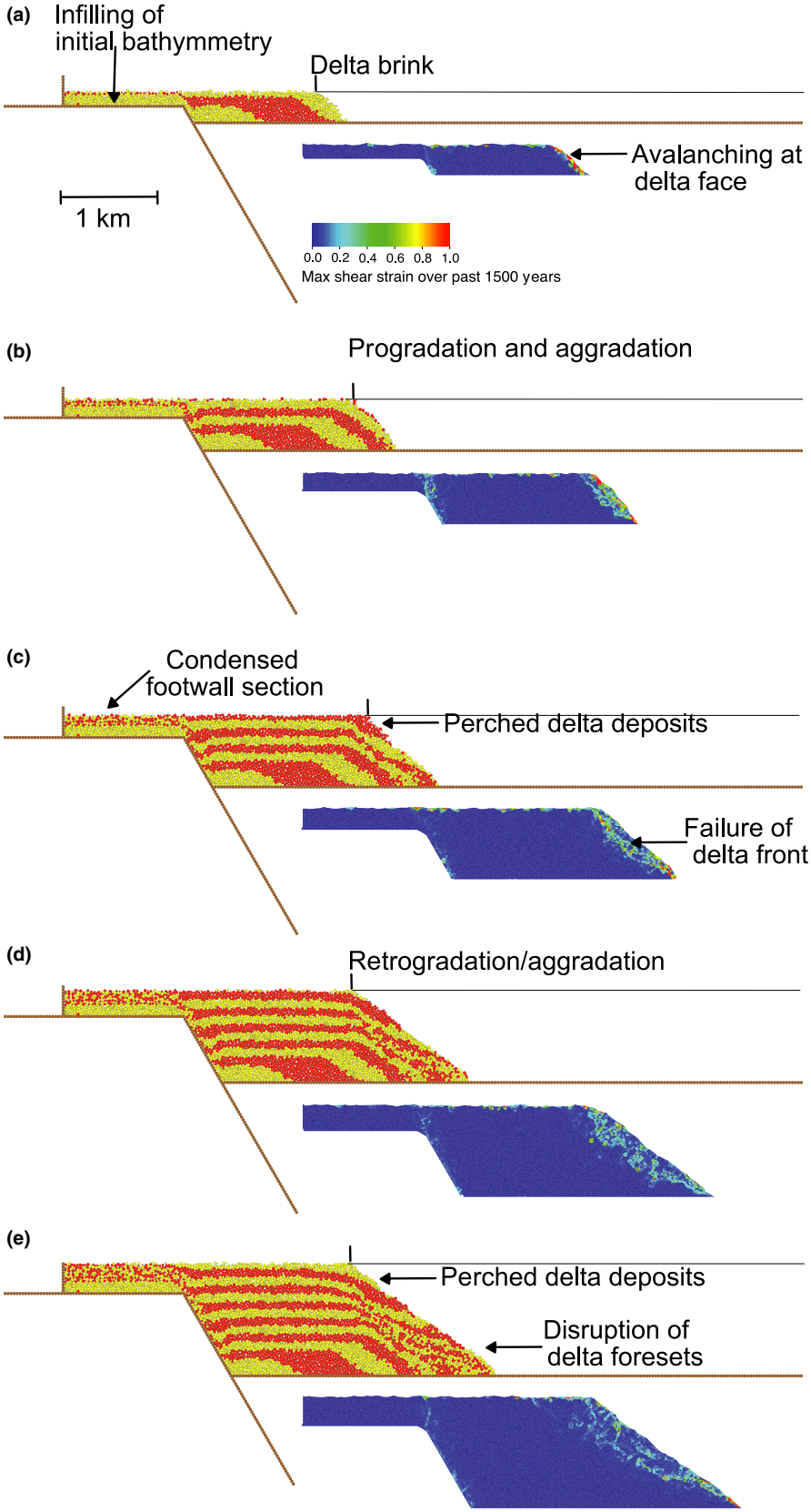

FIGURE 2 A simple footwall-derived Gilbert delta simulation. Model results shown at (a) 100, (b) 200, (c) 300, (d) 400 and (e) 500 ka. Scaled fault slip is 2 m/ka. Also shown is the incremental shear strain over the previous 1,500 years at each stage. Shear strain scale and distance scale shown, no vertical exaggeration

problem of interest. On the one hand, modelling of deformation to high strain is an ideal candidate for the application of the discrete element technique as it is well suited to studying problems in which discontinuities (shear-zones, faults, fractures, etc.) are important. It also allows deformation involving unlimited relative motions of individual elements and complex, abrupt and changing boundary conditions (Cundall & Strack, 1979; Egholm,

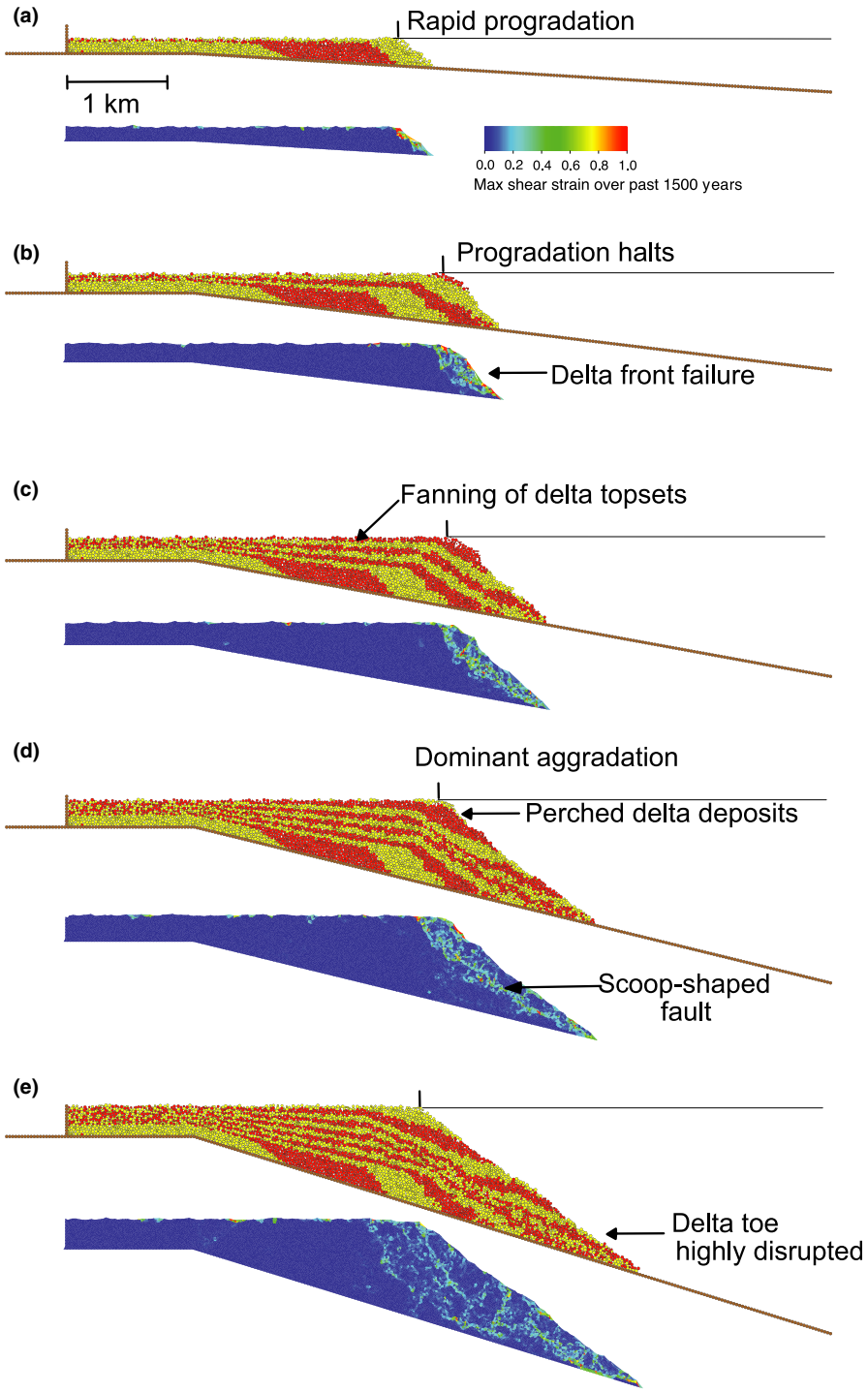

FIGURE 3 A hangingwall-derived Gilbert delta simulation. Model results shown at (a) 100, (b) 200, (c) 300, (d) 400 and (e) 500 ka. Final tilt of initial surface is approximately 17°. Basal surface is frictional. Also shown is the incremental shear strain over the previous 1,500 years at each stage. Shear strain scale and distance scale shown, no vertical exaggeration. Short vertical lines in all model figures show the horizontal position of the delta brink at each stage of model development

Sandiford, Clausen, & Nielsen, 2007; Finch, Hardy, & Gawthorpe, 2004; Hardy, 2008, 2011; Thompson, Bennett, & Petford, 2010). However, one disadvantage of the technique lies in the necessary calibration of micro-particle parameters to emergent physical properties (cf. Botter et al., 2014; Egholm et al., 2007). In a similar manner, the sensitivity of models results to subtle initial differences in, for example, assembly packing is well-known (cf. Abe, van Gent, & Urai, 2011). The interactions of many tens of thousands of particles, both locally and globally, also leads to situations wherein our ability to explain precisely why a particular fault or fracture grew at the expense of a neighbouring one is limited. Such issues also exist in analogue modelling where repeated experiments under the same boundary conditions are reasonably reproducible but not in the finer details of the fault and fracture systems (e.g., van Gent, Holland, Urai, & Loosveld, 2010). Computational limitations on element size and/or model resolution, whilst important previously, are now no longer a particular concern due to recent

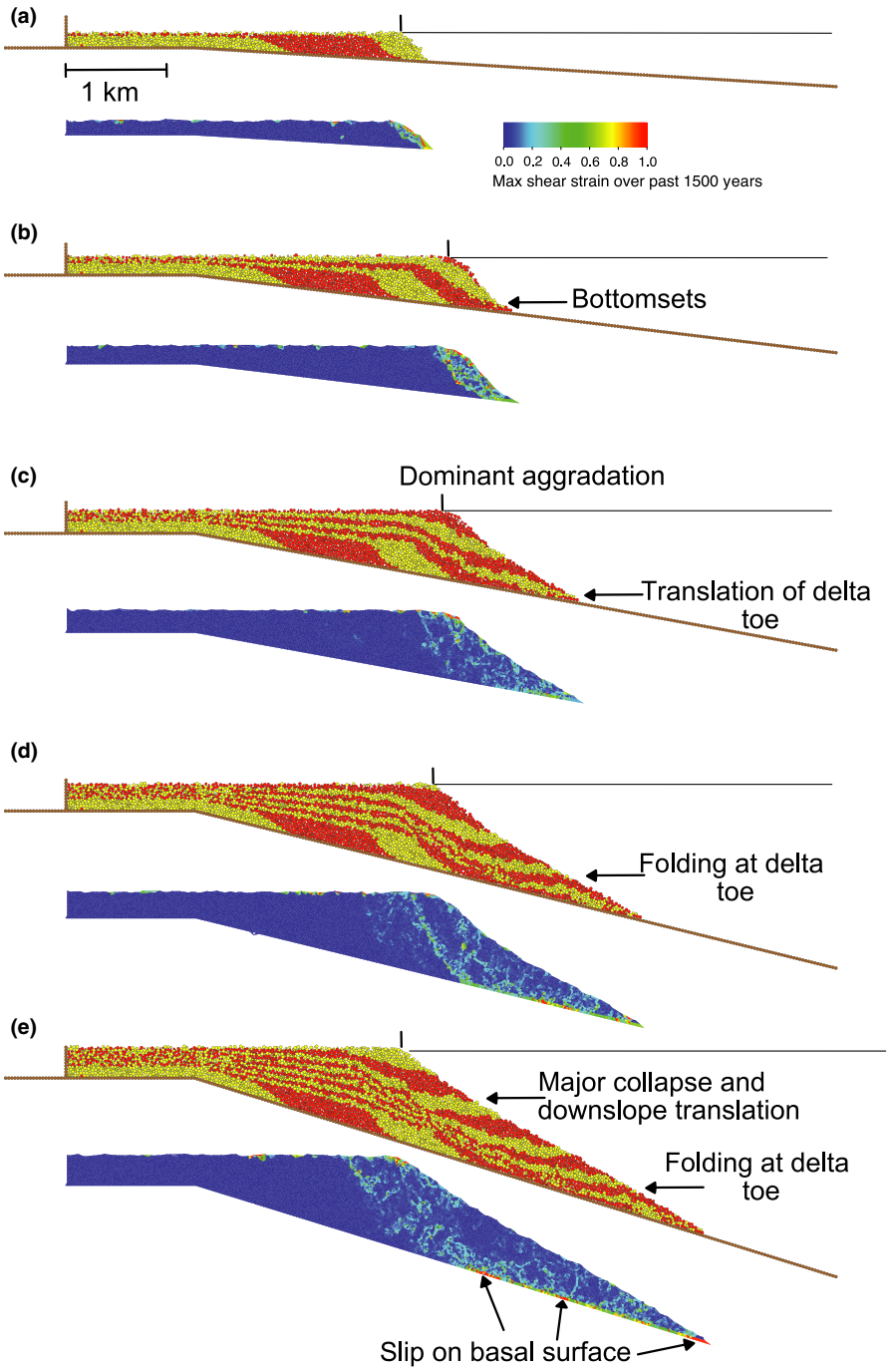

FIGURE 4 A second hangingwall-derived Gilbert delta simulation, but with a frictionless basal, tilting surface. Model results shown at (a) 100, (b) 200, (c) 300, (d) 400 and (e) 500 ka. Final tilt of initial surface is approx. 17°. Also shown is the incremental shear strain over the previous 1500 years at each stage. Shear strain scale and distance scale shown, no vertical exaggeration

rapid advances in computational power and the parallelisation of many discrete element codes.

The discrete element model described here is a variant/development of the lattice solid model (LSM) (Mora & Place, 1993, 1994; Place, Lombard, Mora, & Abe, 2002). A rock, or sedimentary, mass is treated as an assemblage of circular elements, which interact as if connected by breakable elastic springs (bonds) and that undergo motion relative to one another. In this particular application of the modelling technique, I assume that the sedimentary medium under consideration is cohesionless, and thus, all bonds/springs are initially broken. However, for completeness, I will present a full explanation of the modelling approach with bonding (cohesion) included. The behaviour of the elements assumes that the particles interact through a "repulsive–attractive" force (Mora & Place, 1993) in which the resultant (normal) force, F_n, is given by

$$\begin{aligned} F_n &= K_n(r-R) \quad r < r_0 \text{ intact bond} \\ F_n &= K_n(r-R) \quad r < R \text{ broken bond} \\ F_n &= 0 \quad r \geq R \text{ broken bond} \end{aligned} \tag{1}$$

Here, K_n is the elastic constant (normal spring stiffness) of the bond, R is the equilibrium distance between the

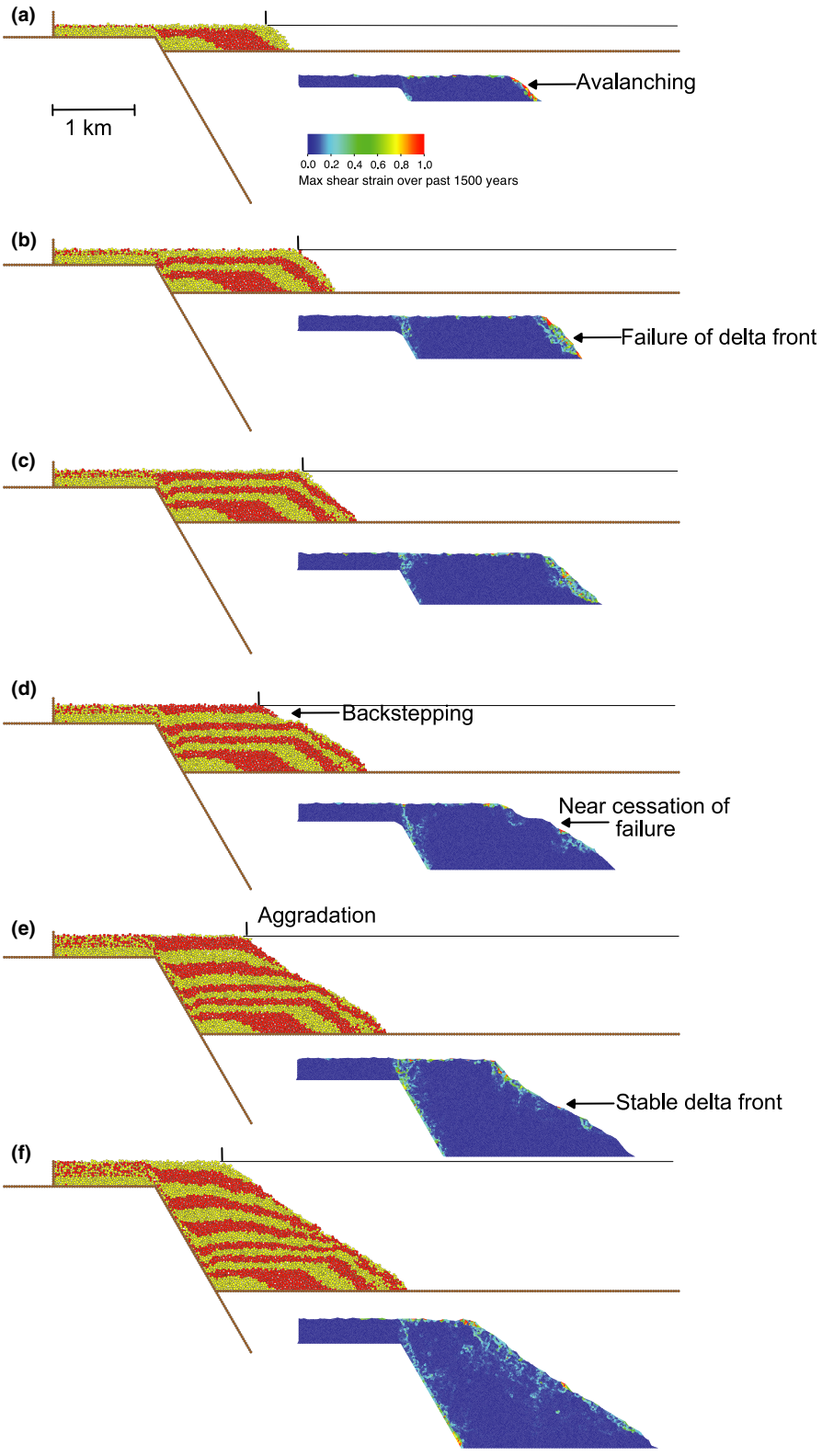

FIGURE 5 A simple footwall-derived Gilbert delta simulation in which the slip rate doubles from 2.0 to 4.0 m/ka at 250 ka. Model results shown at (a) 100, (b) 200, (c) 250, (d) 300, (e) 400 and (f) 500 ka. Also shown is the incremental shear strain over the previous 1,500 years at each stage. Shear strain scale and distance scale shown, no vertical exaggeration

particles (sum of particle radii), r_0 is a breaking threshold, and r is the current distance between the particle pair. Particles within the model assemblage are bonded until the distance (r) between them exceeds the defined breaking threshold at which time the bond breaks. The force acting on a bond at this threshold represents the force necessary for a bond to fail or yield, or, alternatively, can be cast as the stress acting on a particle's bond at failure. After this breaking threshold, the particle pair experiences no further attractive force and the bond is irreversibly broken. However, if the two particles return to a compressive contact, a repulsive force still acts between them. For a cohesionless

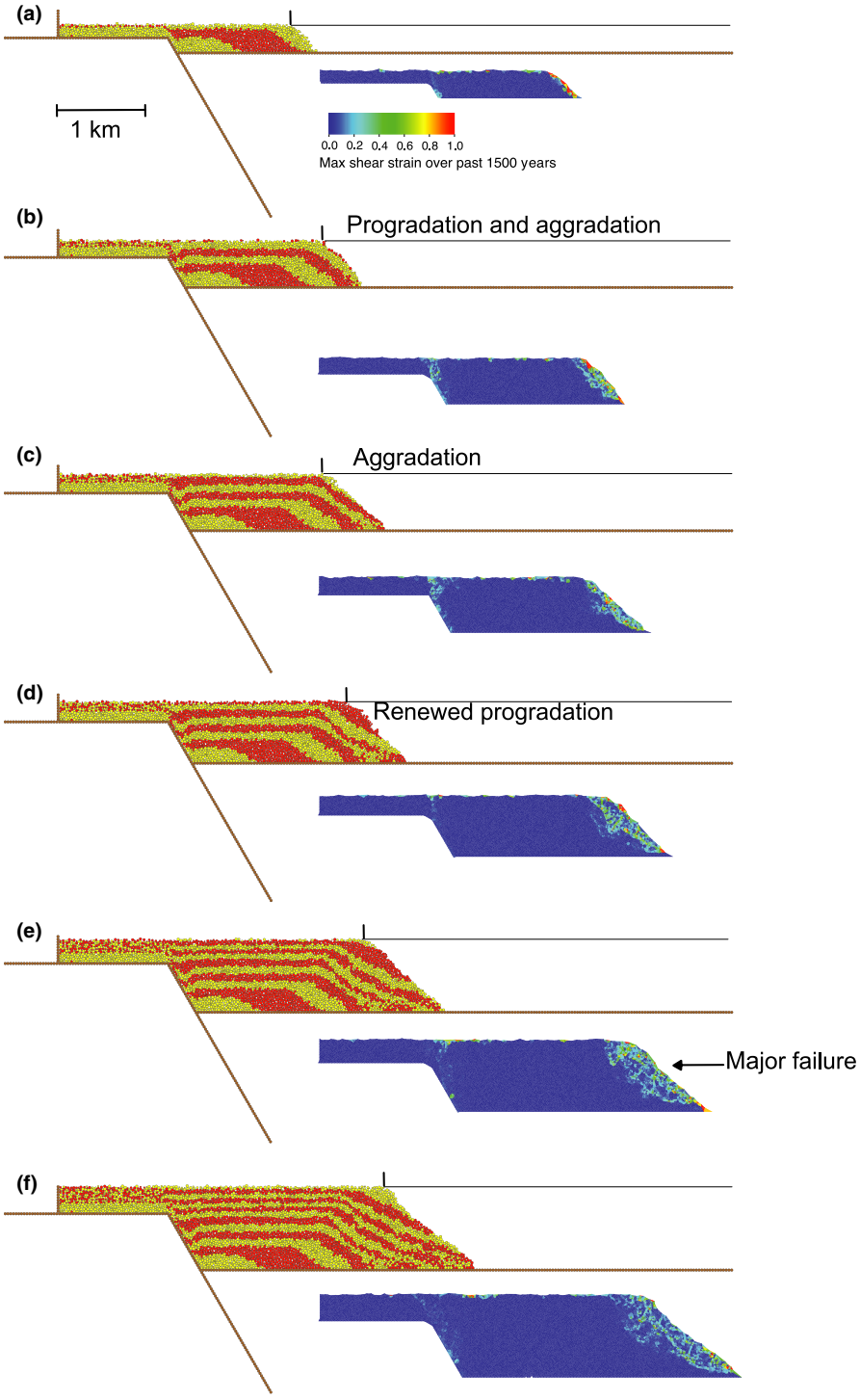

FIGURE 6 A simple footwall-derived Gilbert delta simulation in which the slip rate halves from 2.0 to 1.0 m/ka at 250 ka. Model results shown at (a) 100, (b) 200, (c) 250, (d) 300, (e) 400 and (f) 500 ka. Also shown is the incremental shear strain over the previous 1,500 years at each stage. Shear strain scale and distance scale shown, no vertical exaggeration

material, like the sediments considered herein, all bonds are considered to be initially broken, and thus, only the repulsive part of this elastic force is applied if appropriate.

In addition to treating the normal force (F_n) between particles, I also calculate the tangential (shear) force, F_S, as a result of displacement perpendicular to the vector connecting the particles' centroids. This frictional force acts in a direction opposite to that of the relative tangential velocity and is modelled as a threshold-limited elastic spring in parallel with that used to calculate the normal forces (cf. Cundall & Strack, 1979; Mora & Place, 1994). The magnitude of this force is limited to be less than or equal to the shear force allowed by Coulomb friction:

$$\begin{aligned} F_s &= K_s X_s \\ F_{s\max} &= \mu F_n \\ F_s &= F_{s\max} (\text{if } F_s > F_{s\max}) \end{aligned} \tag{2}$$

where, K_s is the elastic constant (shear spring stiffness) of the contact, $F_{S\max}$ is the maximum (limiting) shear

(frictional) force, F_n is the normal force at a contact and μ is the inter-particle coefficient of friction. If a contact is "lost" between two touching elements (i.e., they separate), then all the forces between the elements are set to zero. The total elastic force, $F_{i,a}$ exerted on a particle is thus obtained by summing the normal and tangential forces on each contact/bond that links a specific particle to its a neighbours (Figure 2b), calculated by

$$F_{i,\alpha} = \sum_{j=1,\alpha} f_{i,j} \quad (3)$$

where, $f_{i,j}$ is the elastic force (normal and shear) experienced by particle i from its neighbouring particle j. However, we include a viscous damping term (proportional to particle velocity) that acts to dampen reflected waves from the rigid edges/boundaries of our model, preventing a build-up of kinetic energy within the closed system (cf. Mora & Place, 1994; Place et al., 2002).

Finally, gravitational forces, F_g, acting on each element are calculated in the z direction. Therefore, the total force (F) on any particle is given by

$$F = F_{i,\alpha} - v\dot{x} + F_g \quad (4)$$

where, v represents the dynamic viscosity and x is the velocity of the particle. At each discrete time step, the particles are advanced to their new positions within the model by integrating their equations of motion using Newtonian physics and a velocity-Verlet-based scheme (Allen & Tildesley, 1987).

The novel approach presented here is the use of the discrete element technique not *only* to model deformation of a pre-existing sedimentary sequence but also to model the deposition of the sedimentary sequence *itself* during active tectonics. The modelling code is basically identical to that previously published/presented except that the sedimentary body being deformed and monitored grows through time as elements are added to it, simulating the accretion of new sediments to a pre-existing, growing delta. In a sense, then, all elements are *growth strata*. The fundamental algorithmic difference in the model presented here is the heuristics of adding a packet of sediments to the pre-existing sequence. All other numerical techniques and approaches used on the elements are identical to those discussed in previous papers to which the interested reader is referred (e.g., Hardy, 2011, 2015; Hardy et al., 2009). In most other sedimentary geometric/numerical models, there is no intrinsic mechanical behaviour to the modelled sediments, and thus, no faulting, folding or collapse/slumping can occur (e.g., Hardy et al., 1994; Ritchie et al., 2004a,b). Here, however, the elements representing the coarse-grained deltaic sediments can have an intrinsic coefficient of friction, cohesion or any other material property appropriate to the system being considered. This allows flow, localisation and internal deformation to develop and thus the mechanics of the deposited sediments are expressed as the delta grows. This is analogous to the difference between geometric/kinematic and mechanical models of fault/fold development; the geometric or kinematic models produce intuitively pleasing and straightforward results, yet they tell you very little about the physics or mechanics of what is actually happening within the structure.

The approach used here is to start with no discrete elements at all, only a pre-existing marine or lacustrine basin with a predefined bathymetry. To this system, a small package of discrete elements is added, at a predefined interval, based on some appropriate heuristic, this means the elements could be deposited in any available submarine accommodation space starting at the shoreline, or they could be deposited uniformly/nonuniformly beneath a defined wave base to simulate basinal sedimentation or even carbonate sedimentation. The actual heuristic is not of great concern here, rather the notion that coarse sediments are added incrementally. After their addition, and careful placement on a pre-existing basinal surface or growing delta, these elements must be allowed to equilibrate/adjust to a final, initial deposited state. This is performed by pausing any external boundary movement after discrete element addition for a predefined (very small) number of time-steps until the added elements are in a quasi-static location and effectively stable. The model then continues as before but with a new sediment load added to the system. The specific heuristic used here is to add a fixed volume/area of simple, frictional discrete elements of variable size (average radius c. 7.5 m), from the shoreline filling up any available submarine accommodation space (Figure 1d). These elements are chosen randomly and then added sequentially with each additional element attempting to minimise the remaining accommodation space until the package is used up. After each element is added, the provisional position of the shoreline changes, and thus, subsequent elements will be added in a more seaward direction. They are carefully placed to ensure that they maximise filling of available accommodation space whilst just touching pre-existing deposited elements. I do not consider the transport of these elements above sea level or their erosion in this preliminary study. The spatial resolution chosen here is arbitrary but it is appropriate to introduce the approach, with today's rapid advances in computing power model resolution is becoming less and less of an issue.

3 | MODEL PARAMETERS, SETUP AND BOUNDARY CONDITIONS

Below, I present the results of five simple two-dimensional numerical models (experiments) which illustrate the utility and power of the technique developed herein. I first examine the growth of a Gilbert-type delta developing as a result

of sediment supply from the footwall of a simple basement normal fault dipping at 60° (Figure 2), then two hanging wall-derived Gilbert deltas being deposited onto a tilting basal surface that is either frictional or frictionless (Figures 3 and 4). Finally, I examine two footwall-derived deltas which are subject to an increase and decrease in slip rate, respectively, during the model run (Figures 5 and 6). All models start with an initial bathymetry of 80 m and a small, regional, base level rise is included to emphasise the condensed nature of the topset sequence outside the zone of tectonic subsidence.

As mentioned above, the heuristic used here to simulate coarse-grained, deltaic sedimentation is to periodically add a package (area m^2) of simple frictional discrete elements of variable size sequentially from the current shoreline filling up any available submarine accommodation space (Figure 1d). Element radii range from 6.25 to 15.625 m (average radius 7.71 m) and their density is 2,200 kg/m3. These elements obey Newton's equations of motion and interact with each other under the influence of gravity. Elements are not bonded and only experience Mohr-Coulomb frictional contact interactions with their neighbours (see Finch et al., 2004 and Hardy et al., 2009 for a full description of the modelling approach). In discrete element models, such as that used here the parameters, such as strength and coefficient of friction, of an assemblage are emergent properties and do not relate directly to micro-properties. They are typically assessed through the use of angle of repose and/or unconfined/confined biaxial numerical tests (cf. Botter et al., 2014; Finch et al. 2004; Holohan, Schopfer, & Walsh, 2011; Oger, Savage, Corriveau, & Sayed, 1998). Using such tests, the frictional sedimentary elements used here have been found to have a bulk coefficient of friction (μ) of c. 0.70 (internal angle of friction (ϕ) of c. 35°) and have no cohesion. These values lie within the ranges reported for natural rock masses (cf. Holohan et al., 2011; Schultz, 1996; Strayer, Erickson, & Suppe, 2004) and are appropriate for modelling a frictional, granular unlithified sedimentary body. They are also chosen here to illustrate that the approach presented here can handle extreme delta slopes and their subsequent collapse, rather than to assert that all Gilbert delta forests are equally as steep. There are no stability issues with such steep slopes.

The applied basement fault displacement or hanging-wall tilt in each experiment is transmitted to the growing delta, changing local element interactions and thus contact forces. As a result of the change in local forces, the internal elements are advanced to their new positions within the model by integrating their equations of motion using Newtonian physics and a velocity-Verlet based numerical scheme (cf. Mora & Place, 1993). Element positions are saved during experiments to allow a detailed, high-resolution analysis of geometry, displacement and strain (cf. Cardozo & Allmendinger, 2009). The numerical code used (cdem2D) has been parallelised using OpenMP and has been thoroughly tested and verified against the serial version (cf. Chapman, Jost, & van der Pas, 2007; Hardy, 2015). Typical experiments like those discussed here take ~1–2 days to run on a desktop machine with two 6-core Intel Xeon (X5650 – 2.66 GHz) processors allowing 24 computational threads. The final deltas in each experiment are composed of approximately 20,000 elements.

Models are run for c. 0.46 days of model time, which I choose to scale to c. 0.5 Ma of real geological time, appropriate for large, Gilbert-type deltas associated with major normal faults (cf. Backert et al., 2010; Hardy & Gawthorpe, 2002). This means that the displacement rates used scale to 0.5–4.0 m/ka, well within reported fault displacement rates (see Hardy, 1994). In the case of the tilting hanging-wall model, approximately 17° of tilt is achieved during the 500 ka of model run time. The small, regional, base level rise included in the modelling scales to c. 0.4 m/ka. In all cases, the modelled sediment supply equates to approximately 5,000 m^2/ka, and the sediments are marked/coloured according to (time) packets of deposition (c. 40 ka) to emphasise the evolving stratigraphy and deformation styles. Model results are presented at regular intervals throughout as "time snapshots," along with the incremental shear strain over the previous 1,500 years to observe the internal deformation within the growing sedimentary body.

For each experiment discussed herein, many different models have been run with parameters similar to those described above. However, the specific experiments discussed are representative of the stratigraphic and structural evolution typically observed under these boundary conditions in that they contain the reproducible, characteristic features seen in many models. The important scientific message to be taken away is not the precise location of an individual geometric feature or fault, but rather the distinctive, reproducible structural behaviour and stratigraphic sequences that emerge from multiple experiments.

4 | NUMERICAL EXPERIMENT RESULTS

4.1 | Experiment 1: footwall-derived Gilbert delta, simple normal fault

In this model, the simplest presented herein, a basement normal fault dipping at 60° slips at 2 m/ka over 500 ka, giving a total fault slip of 1 km. Thus, accommodation for the supplied sediments is mainly provided by hanging-wall subsidence (Figure 2). After 100 ka (equivalent to 200 m of displacement on the basement fault), a very simple sedimentary package has developed. It reflects both the infilling of the initial bathymetry (80 m) and fault-controlled

accommodation space. The small delta that is developed in the hanging wall of the fault dominantly exhibits progradation with some aggradation (Figure 2a), also note that even at this stage, early delta deposits are faulted and offset across the basement fault. The foresets dip on average at c. 30–35°. True bottomsets are practically absent in this delta with the steep foresets down-lapping on the seafloor (cf. Figure 1a). At this stage, the shear strain plot shows that deformation is restricted to the immediate delta face/slope, internally the delta is essentially undeformed. This postdeposition deformation reflects the avalanching of elements downslope as the delta brink over-steepens periodically and exceeds the discrete elements stable angle of repose (c. 35°). After 200 ka (400 m displacement), there is an obvious decrease in the rate of progradation but the delta continues to aggrade (observe the topset breakpoint trajectory in Figure 2b). As the delta has grown in both thickness and foreset height, deformation is now more widespread at the delta front with external avalanching and internal failure visible. Deformation is also present adjacent to and above the basement fault (Figure 2b). After 300 ka (600 m displacement), the delta has become dominantly aggradational with limited progradation (Figure 2c) and from the shear strain plot, a scoop-shaped fault or slip surface can be seen to have developed. It is interesting that the downslope movement on this surface (slumping) generates additional accommodation space at the delta front leading to the development of infilling perched delta deposits (Figure 2c). After 400 ka (800 m displacement), retrogradation starts to occur as sediment supply cannot compete with accommodation due to hanging-wall subsidence and additional slumping at the delta front (Figure 2d; cf. Figure 1b) and consequently little sediment arrives at the delta front. Due to this faulting and slumping/downslope movement, older foresets start to be disrupted at the toe of the delta. Avalanching on the immediate delta front surface almost ceases but internal deformation on large scoop-shaped slip surfaces continues (Figure 2d). After 500 ka (1,000 m displacement), aggradation with minor retrogradation continues and there are notable disruption and faulting of previously deposited foresets due to downslope slumping and collapse (Figure 2e). Note that the basement fault has propagated up into the Gilbert delta cutting and offsetting the topsets, highlighting the condensed nature of the footwall sequence (Figure 2e). Overall, this basic model produces early, rapid progradation followed by dominant aggradation and eventual retrogradation, very similar to previous geometric models (cf. Hardy et al., 1994; Figure 1c). The incremental shear strain plots show that much of this delta body remains undeformed after sediment deposition, the exceptions being in the region adjacent to the basement fault and its extension into the cover, and a broad region at the delta front due to loading and collapse later in the evolution of the delta. Above the basement fault, incremental deformation (shear strain) in cover varies quite markedly (cf. Fig 2b–e). This is as a result of subtle changes in contact forces as a result of dilation, relative particle movement and a changing load, all of which lead to nonconstant localisation particularly at such shallow depths.

4.2 | Experiment 2: hanging wall-derived delta, progressive tilt with frictional base

This model has an identical initial bathymetry (80 m) and sediment supply to Experiment 1, the only difference now is that there is no basement fault but rather we simulate a hanging wall that undergoes a simple progressive tilt about a fixed horizontal axis or hinge line (represented as a hinge point in 2D cross-section view) (Figure 3). The final amount of tilt is approximately 17°. After 100 ka (c. 3.4° of tilt), a very simple sedimentary package has developed. It reflects the infilling of initial bathymetry and exhibits dominant progradation with some aggradation (Figure 3a), progradation at this stage is rapid as less accommodation is created than in the fault-controlled model (cf. Figure 2a). The delta has foresets that dip on average at c. 30–35° and, as before, true bottomsets are practically absent with foresets down-lapping on the seafloor (cf. Figure 1a). The shear strain plot shows that deformation is essentially restricted to the delta slope, internally the delta appears undeformed. After 200 ka (c. 6.8° of tilt), there is an obvious decrease in the rate of progradation (Figure 3b). Note the fanning of topsets in a basinward direction due to the ongoing hanging-wall tilt. As the delta grows both in thickness and foreset height, the delta slope continues to fail, but as the tilting takes place continually over-steepening the delta front, deformation is quite widespread (Figure 3b). After 300 ka (c. 10.2° of tilt), the delta is becoming aggradational (Figure 3c) and from the shear strain plot, a scoop-shaped fault/slip surface can be seen at the delta front. After 400 ka (c. 13.6° of tilt), the delta becomes dominantly aggradational as sediment supply is insufficient to fill all of the accommodation created by basinward tilt and downslope movement at the delta front (Figure 3d). This slumping generates additional accommodation space leading to the development of infilling perched delta deposits (Figure 3d). In addition, due to slumping and faulting earlier foresets are beginning to be disrupted. After 500 ka (c. 17° of tilt), we observe continued aggradation and more disruption of foreset coherence due to continued slumping and collapse (Figure 3e). There are now multiple slip surfaces within the delta causing much internal disruption of pre-existing geometries. The incremental shear strain plot shows that much of this delta basinward of the topset-foreset transition is deformed as it

is continually over-steepened, with the development listric scoop-shaped fault surfaces and sub-horizontal slip surfaces at the deepest levels of the delta. There is only limited slip along the basal surface as, in this experiment, this surface is frictional.

4.3 | Experiment 3: hanging wall-derived delta, progressive tilt with frictionless base

In this model, we have an identical setup to Experiment 2, with the only difference that we now introduce a frictionless basal surface to test the effect of friction upon both delta evolution and internal deformation. After 100 ka, as before, a very simple sedimentary package has developed, reflecting both the infilling of the initial bathymetry and hanging-wall tilting. It exhibits rapid progradation with some aggradation (Figure 4a). At this stage, bottomsets are practically absent with foresets down-lapping on the basin floor. The shear strain plot shows that deformation is essentially restricted to the delta slope, internally the delta is undeformed. After 200 ka, there is an obvious decrease in the rate of progradation and the delta starts to aggrade (Figure 4b). As the delta grows in thickness and height, deformation occurs more generally as the delta front begins to fail, but more importantly the continual hanging-wall tilting over-steepens the delta front. As in Experiment 2, bottomsets are beginning to be developed due to failure and transport of sediments downslope, leading to more sigmoidal clinoform geometries (Figure 4b, cf. Figure 3b). Up to this stage, the evolution of Experiments 2 and 3 is quite similar, but from now on they diverge as the influence of the frictionless lower boundary becomes marked. After 300 ka, there is the beginning of more dominant aggradation (Figure 4c) and from the shear strain plot deformation is seen to be quite widespread in the region of the delta front (Figure 4c), note also the translation of the delta toe downslope. At 400 ka, the delta geometry changes markedly (Figure 4d). There is no major internal deformation and disruption of the delta with translation of material downslope, via both internal faulting and slip on the basal (frictionless) surface. In addition, we can now observe the development of faulting, folding and thrusting at the delta toe. After 500 ka, there is now much folding at the delta toe, as a result of major collapse and downslope translation of a large part of the delta front (Figure 4e). We see that, in general, much of this delta is highly deformed with significant translation of sediments downslope via slip along the basal, frictionless and surface.

4.4 | Experiment 4: footwall-derived Gilbert delta with increase in fault slip rate

In this model, we have an identical setup to Experiment 1, the only difference being that halfway through the model run time, at 250 ka, we now *double* the slip rate on the basement normal fault from 2.0 m/ka to 4.0 m/ka. All other model parameters are unchanged. Delta geometries at 100 and 200 ka are identical to those of Experiment 1, and will not be discussed further here but are shown for completeness (Figure 5a,b). Figure 5c shows the state of the delta exactly at the moment (250 ka) when the slip rate is about to double. Here, a simple delta with steep foresets and a progression from dominant progradation to dominant aggradation is seen, with notable failure of the delta front. However, at 300 ka, after the increase in slip rate, we see a strikingly different delta geometry (Figure 5d). As a result of the increased hanging-wall accommodation created by increased fault slip but an unchanged sediment supply, the delta has backstepped dramatically and the active delta front is now situated above older topset deposits. Thus, sediment deposition no longer occurs at the previous delta front. However, more interestingly, this backstepping has an unexpected effect on the previous delta front and slope. As the older delta front and slope are no longer being loaded by the deposition of new sediments due to backstepping, they quickly assume a basically stable geometry and slumping and failure almost cease (Figure 5d). After 400 ka, the delta has continued to grow through aggradation, and the (previous) delta front remains essentially stable (Figure 5e). The new delta front, the locus of active sedimentation, can be seen to be over-steepening, leading to avalanching at the delta slope. At 500 ka, this style of delta evolution continues, although internal failure of the delta front begins to occur once more as the height and length of the delta front grows and upslope loading grows (Figure 5f).

4.5 | Experiment 5: footwall-derived Gilbert delta with decrease in fault slip rate

In this model, we also have an identical setup to Experiment 1, the only difference being that halfway through the model run time, at 250 ka, we now *halve* the slip rate from 2.0 m/ka to 1.0 m/ka. All other model parameters are unchanged. Delta geometries at 100 and 200 ka are identical to those of Experiment 1, and will not be discussed here but are shown for completeness (Figure 6a,b). Figure 6c shows the state of the delta exactly at the moment (250 ka) when the slip rate is about to halve. As before, a simple delta with steep foresets and a progression from dominant progradation to dominant aggradation is seen, with notable failure of the delta front. However, at 300 ka, after the decrease in slip rate, we see a strikingly different delta geometry (Figure 6d). As a result of the decreased hanging-wall accommodation created by lower fault slip but an unchanged sediment supply, the delta has returned to progradation and the active delta front is now situated

above older foreset deposits (observe the topset breakpoint trajectory in Figure 6d). However, more interestingly, this progradation has a dramatic effect on the previous delta front, as it is now being loaded by an increased volume of sediments with the result that faulting and downslope transport are reinvigorated (Figure 6d). This can be seen in the shear strain plot where a broad region of the delta front shows failure. At both 400 and 500 ka, we observe that the delta continues to grow through dominant progradation, and that the delta front is essentially unstable with major failure occurring on scoop-shaped slip surfaces (Figure 6e,f).

5 | DISCUSSION AND CONCLUSIONS

This study presents initial results from a novel, discrete element, approach to the 2D numerical modelling of coarse-grained, Gilbert-type, deltas. It has been applied here to an extensional tectonic setting with continual relative base level rise. In one sense, it is similar to previous geometric/numerical models of Gilbert deltas in that it reproduces their basic geometric features, and has examined the effect of tectonics on accommodation and thus delta stacking patterns (cf. Hardy & Gawthorpe, 1998, 2002; Hardy et al., 1994). However, the experimental results presented here are also strikingly *different* to previous geometric/numerical models of such sedimentary systems in a number of aspects. Firstly, faulting, slumping, downslope movement of sediments and folding all develop naturally within the growing delta body, as a result of the local, and changing, balance of forces within the system. Thus, once deposited, the sedimentary packages in this model are not just passive, geometric markers (compare Figure 1c and Figure 4e), they are affected by ongoing sedimentation (loading) and/or over-steepening of the delta front. As a result, the discrete elements can be subject to avalanching down the active delta front/face and basinward movement and translation on internal slip surfaces. Second, there is a clear feedback between failure/collapse near the current, active delta front, creation of additional accommodation space at this location, subsequent sedimentation and further sediment loading. Third, a variety of different boundary conditions can be applied and their effects on internal deformation and delta geometry assessed, in this case, we have examined the impact of having a simple normal fault and a tilting hanging-wall with or without friction, but many other scenarios are possible. Fourth, and perhaps most importantly, the stratigraphic architectures developed, under even simple boundary conditions, are much more complex than those developed by previous geometric/numerical models of equivalent deltas.

Whilst these results are provisional they do highlight some key issues that may arise in the analysis and interpretation of Gilbert-type delta stratigraphies observed in nature: (a) There are a variety of different processes that occur in space and time as the modelled deltas develop. When the modelled deltas are small, movement of coarse-grained sediment downslope is dominantly via avalanching at the delta face/front due to sediment delivery and over-steepening at the delta brink. However, as the modelled delta bodies grow in thickness/foreset length, major internal deformation becomes more likely due to loading, failure and movement on scoop-shaped slip surfaces. Thus, a small, relatively thin, delta may have a quite different geometry and exhibit very different instability features compared to a larger, thick delta; (b) The interpretation of topset breakpoint trajectories in Gilbert deltas is clearly useful but can be subject to difficulties when faulting, slumping and downslope sediment transport occur in the region of the delta front. It is precisely in the region of the topset-foreset transition that *local* accommodation space is created, and thus, interpretation of *subtle* changes in topset breakpoint trajectories in terms of eustasy and/or basement fault activity can be problematic; (c) Changes in accommodation as a result of varying rates of basement fault slip do not only affect delta stacking patterns (progradation, aggradation or retrogradation), but they can also have a direct impact upon the location and intensity of deformation within the delta. Backstepping of the delta as a result of *increased* fault slip not only reduces sediment supply to the previous delta front, but also causes a cessation of delta front failure as the location of sedimentary loading of pre-existing deposits changes. Progradation as a result of *decreased* fault slip not only increases sediment supply to the previous delta front and renewed progradation, but also causes an increase in delta front failure as the amount of sedimentary loading of pre-existing deposits increases.

The initial results shown here are, in a sense, proof of concept. They have been chosen to illustrate the potential of the proposed technique and the manner in which it can encapsulate some of the processes active in Gilbert-type deltas. Here, an extensional tectonic setting has been presented but a contractional setting could easily be handled in the same manner. The idea has been to show how *different* modelled delta geometries can be if one includes *mechanics* in their description and they are not just treated as simple passive sedimentary markers. Here, I have used the incremental shear strain to illustrate internal, incremental deformation but given the discrete nature of the sediments, it is relatively easy to calculate and display extension, shortening, rotation or dilation.

The models presented here are by no means complete, but show the power of the technique. There are many additional features or mechanical properties that could be added

depending on the geological scenario being considered, for example, (a) A first-level limitation is the lack of any sediment transport above sealevel to the delta and the lack of erosion below sealevel or during base level fall; these are not fundamental limitations of the model. (b) The sediments modelled here have uniform mechanical properties, and the addition of a (spatial or temporal) variation in element properties within the introduced sediments would clearly have a major impact upon their behaviour. (c) It is similar that the addition of deeper water, "suspension" prodelta elements with their own physical properties would be straightforward. (d) The elements in the models presented here are coloured according to their timeframe of deposition—there is no a priori reason that they cannot be coloured by the information that they carry with them, be that initial depth of deposition, distance from shoreline, etc. (e) The approach presented here does not consider early lithification of delta deposits (or carbonates) but this could easily be included by allowing elements to have or develop cohesion or bonding after a given amount of time or burial depth. These and other topics are subjects of ongoing research.

ACKNOWLEDGEMENTS

Discussions with, and the patience of, many colleagues over many years is appreciated; thanks must go particularly to Dave Waltham for stimulating my interest in modelling sedimentation many years ago. Ana Carmona also must be thanked for reawakening my interest in modelling sediments. Comments of Editor Rebecca Bell and Reviewers Rebecca Dorsey and Guillaume Duclaux were helped greatly to improve the manuscript. Discrete element modelling was carried out using cdem2D by the author and strain analysis carried out using SSPX by Nestor Cardozo. Anyone who wishes access to cdem2D or collaboration is welcome to contact the author.

REFERENCES

Abe, S., van Gent, H., & Urai, J. L. (2011). DEM simulation of normal faults in cohesive materials. *Tectonophysics*, *512*, 12–21. https://doi.org/10.1016/j.tecto.2011.09.008

Allen, M. P., & Tildesley, D. J. (1987). *Computer simulation of liquids*. Oxford, UK: Oxford Science Publications.

Backert, N., Ford, M., & Malartre, F. (2010). Architecture and sedimentology of the Kerinitis Gilbert-type fan delta, Corinth Rift, Greece. *Sedimentology*, *57*, 543–586. https://doi.org/10.1111/j.1365-3091.2009.01105.x

Botter, C., Cardozo, N., Hardy, S., Lecomte, I., & Escalona, A. (2014). From mechanical modeling to seismic imaging of faults: A synthetic workflow to study the impact of faults on seismic. *Marine and Petroleum Geology*, *57*, 187–207. https://doi.org/10.1016/j.marpetgeo.2014.05.013

Botter, C., Cardozo, N., Hardy, S., Lecomte, I., Paton, G., & Escalona, A. (2016). Seismic characterisation of fault damage in 3D using mechanical and seismic modelling. *Marine and Petroleum Geology*, *77*, 973–990. https://doi.org/10.1016/j.marpetgeo.2016.08.002

Cardozo, N., & Allmendinger, R. W. (2009). SSPX: A program to compute strain from displacement/velocity data. *Computers & Geosciences*, *35*, 1343–1357. https://doi.org/10.1016/j.cageo.2008.05.008

Chapman, B., Jost, G., & van der Pas, R. (2007). *Using OpenMP: Portable shared memory parallel programming*. Cambridge, MA: The MIT Press.

Colella, A. (1988a). Fault-controlled marine Gilbert-type fan deltas. *Geology*, *16*, 1031–1034. https://doi.org/10.1130/0091-7613(1988)016<1031:FCMGTF>2.3.CO;2

Colella, A. (1988b). Pliocene-Holocene fan deltas and braid deltas in the Crati Basin, southern Italy: A consequence of varying tectonic. In W. Nemec, & R. J. Steel (Eds.), *Fan deltas: Sedimentology and tectonic settings* (pp. 50–74). Blackie and Son: Glasgow and London.

Cundall, P. A., & Strack, O. D. L. (1979). A discrete numerical model for granular assemblies. *Geotechnique*, *29*, 47–65. https://doi.org/10.1680/geot.1979.29.1.47

Dart, C. J., Collier, R. E. L., Gawthorpe, R. L., Keller, J. V. A., & Nichols, G. (1994). Sequence stratigraphic of (?)Pliocene- Quaternary synrift, Gilbert-type fan deltas, northern Peloponnesos, Greece. *Marine and Petroleum Geology*, *11*, 545–560. https://doi.org/10.1016/0264-8172(94)90067-1

Egholm, D. L., Sandiford, M., Clausen, O. R., & Nielsen, S. B. (2007). A new strategy for discrete element numerical models: 2. Sandbox applications. *Journal of Geophysical Research*, *112*, B05204. https://doi.org/10.1029/2006JB004558

Fernandez, J., & Guerra-Merchan, A. (1996). A coarsening upward megasequence generated by a Gilbert-type fan-delta in a tectonically controlled context (Upper Miocene, Gua- dix-Baza Basin, Betic Cordillera, southern Spain). *Sedimentary Geology*, *105*, 191–202. https://doi.org/10.1016/0037-0738(95)00137-9

Finch, E., Hardy, S., & Gawthorpe, R. L. (2004). Discrete element modelling of extensional fault-propagation folding above rigid basement fault blocks. *Basin Research*, *16*, 489–506.

Ford, M., Williams, E. A., Malartre, F., & Popescu, S. M. (2007) Stratigraphic architecture, sedimentology and structure of the Vouraikos Gilbert-type fan delta, Gulf of Corinth, Greece. In G. Nichols, E. Williams & C. Paola (Eds.), *Sedimentary processes, environments and basins: A tribute to Peter Friend* (vol. *38*, pp. 49–90). International Association of Sedimentologists Special Publication. Malden, MA: Blackwell Publication. https://doi.org/10.1002/9781444304411

Garcia-Garcia, F., Fernandez, J., Viseras, C., & Soria, J. H. (2006). Architecture and sedimentary facies evolution in a delta stack controlled by fault growth (Betic Cordillera, southern Spain, late Tortorian). *Sedimentary Geology*, *185*, 79–92. https://doi.org/10.1016/j.sedgeo.2005.10.010

van Gent, H. W., Holland, M., Urai, J. L., & Loosveld, R. (2010). Evolution of fault zones in carbonates with mechanical stratigraphy - Insights from scale models using layered cohesive powder. *Journal of Structural Geology*, *32*, 1375–1391. https://doi.org/10.1016/j.jsg.2009.05.006

Gilbert, G. K. (1885). *The topographic features of lake shores*. US Geological Survey Annual Report, *5*, 69–123.

Gilbert, G. K. (1890). *Lake Bonneville*. US Geological Survey Monograph, *1*, 1–438.

Gratacos, O., Bitzer, K., Cabrera, L., & Roca, E. (2009). SIMSAFA-DIM-CLASTIC: A new approach to mathematical 3D forward simulation modelling for terrigenous and carbonate marine sedimentation. *Geologica Acta*, *7*, 311–322.

Hardy, S. (1994). *Mathematical modelling of sedimentation in active tectonic settings*. PhD Thesis, Royal Holloway University of London.

Hardy, S. (2008). Structural evolution of calderas: Insights from two-dimensional discrete element simulations. *Geology*, *36*, 927–930. https://doi.org/10.1130/G25133A.1

Hardy, S. (2011). Cover deformation above steep, basement normal faults: Insights from 2D discrete element modeling. *Marine and Petroleum Geology*, *28*, 966–972. https://doi.org/10.1016/j.marpetgeo.2010.11.005

Hardy, S. (2015). The Devil truly is in the detail. A cautionary note on computational determinism: Implications for structural geology numerical codes and interpretation of their results. *Interpretation*, *3*(4), SAA29–SAA35. https://doi.org/10.1190/INT-2015-0052.1

Hardy, S. (2016). Does shallow dike intrusion and widening remain a possible mechanism for graben formation on Mars? *Geology*, *44*, 107–110. https://doi.org/10.1130/G37285.1

Hardy, S. (2018). Coupling a frictional-cohesive cover and a viscous substrate in a discrete element model: First results of application to thick- and thin-skinned extensional tectonics. *Marine and Petroleum Geology*, *97*, 32–44. https://doi.org/10.1016/j.marpetgeo.2018.06.026

Hardy, S., Dart, C. J., & Waltham, D. (1994). Computer modelling of the influence of tectonics on sequence architecture of coarse-grained fan deltas. *Marine and Petroleum Geology*, *11*, 561–574. https://doi.org/10.1016/0264-8172(94)90068-X

Hardy, S., & Gawthorpe, R. L. (1998). Effects of variations in fault slip rate on sequence stratigraphy in fan deltas: Insights from numerical modeling. *Geology*, *26*, 911–914. https://doi.org/10.1130/0091-7613(1998)026<0911:EOVIFS>2.3.CO;2

Hardy, S., & Gawthorpe, R. L. (2002). Normal fault control on bedrock channel incision and sediment supply: Insights from numerical modeling. *Journal of Geophysical Research*, *107*, 2246. https://doi.org/10.1029/2001JB000166

Hardy, S., McClay, K., & Muñoz, J. A. (2009). Deformation and fault activity in space and time in high-resolution numerical models of doubly vergent thrust wedges. *Marine and Petroleum Geology*, *26*, 232–248. https://doi.org/10.1016/j.marpetgeo.2007.12.003

Holohan, E. P., Schopfer, M. P. J., & Walsh, J. J. (2011). Mechanical and geometric controls on the structural evolution of pit crater and caldera subsidence. *Journal of Geophysical Research*, *116*, B07202. https://doi.org/1029/2010JB008032

Malartre, F., Ford, M., & Williams, E. A. (2004). Preliminary biostratigraphy and 3D geometry of the Vouraikos Gilbert-type fan delta, Gulf of Corinth, Greece. *CR Académie des Sciences, Paris*, *336*, 269–280.

Mora, P., & Place, D. (1993). A lattice solid model for the non-linear dynamics of earthquakes. *International Journal of Modern Physics C*, *4*, 1059–1074. https://doi.org/10.1142/S0129183193000823

Mora, P., & Place, D. (1994). Simulation of the frictional stick-slip instability. *Pure and Applied Geophysics*, *143*, 61–87. https://doi.org/10.1007/BF00874324

Oger, L., Savage, S. B., Corriveau, D., & Sayed, M. (1998). Yield and deformation of an assembly of disks subject to a deviatoric stress loading. *Mechanics of Materials*, *27*, 189–210. https://doi.org/10.1016/S0167-6636(97)00066-5

Place, D., Lombard, F., Mora, P., & Abe, S. (2002). Simulation of the micro-physics of rocks using LSMEarth. *Pure and Applied Geophysics*, *159*, 1911–1932. https://doi.org/10.1007/s00024-002-8715-x

Ritchie, B. D., Gawthorpe, R. L., & Hardy, S. (2004a). Three-dimensional numerical modeling of deltaic depositional sequence 1: Influence of the rate and magnitude of sea-level change. *Journal of Sedimentary Research*, *74*, 203–220. https://doi.org/10.1306/091303740203

Ritchie, B. D., Gawthorpe, R. L., & Hardy, S. (2004b). Three-dimensional numerical modeling of deltaic depositional sequences 2: Influence of local controls. *Journal of Sedimentary Research*, *74*, 221–238. https://doi.org/10.1306/091303740221

Ritchie, B. D., Hardy, S., & Gawthorpe, R. L. (1999). Three-dimensional numerical modeling of coarse-grained clastic deposition in sedimentary basins. *Journal of Geophysical Research*, *104*, 17759–17780. https://doi.org/10.1029/1999JB900170

Schultz, R. A. (1996). Relative scale and the strength and deformability of rock masses. *Journal of Structural Geology*, *18*, 1139–1149. https://doi.org/10.1016/0191-8141(96)00045-4

Strayer, L. M., Erickson, S. G., & Suppe, J. (2004). Influence of growth strata on the evolution of fault-related folds: Distinct-element models. In M. & K. (Ed.), *Thrust Tectonics and Hydrocarbon Systems*. Tulsa, OK: American Association of Petroleum Geologists Memoir 82 (pp. 413–437).

Thompson, N., Bennett, M. R., & Petford, N. (2010). Development of characteristic volcanic debris avalanche deposit structures: New insights from distinct element simulations. *Journal of Volcanology and Geothermal Research*, *192*, 191–200.

How to cite this article: Hardy S. Novel discrete element modelling of Gilbert-type delta formation in an active tectonic setting—first results. *Basin Res*. 2018;00:1–15. https://doi.org/10.1111/bre.12309